

Ni_xFe_{1-x}B Nanoparticles Self-Modified Nanosheets as Efficient Bifunctional Electrocatalysts for Water Splitting: Experiments and Theories

*Weizhao Hong, Shanfu Sun, Yi Kong, Yongyuan Hu, Gang Chen**

W. Hong, S. Sun, Y. Kong, Y. Hu and Prof. G. Chen, MIIT Key Laboratory of Critical Materials Technology for New Energy Conversion and Storage, School of Chemistry and Chemical Engineering, Harbin Institute of Technology, Harbin, P. R. China.

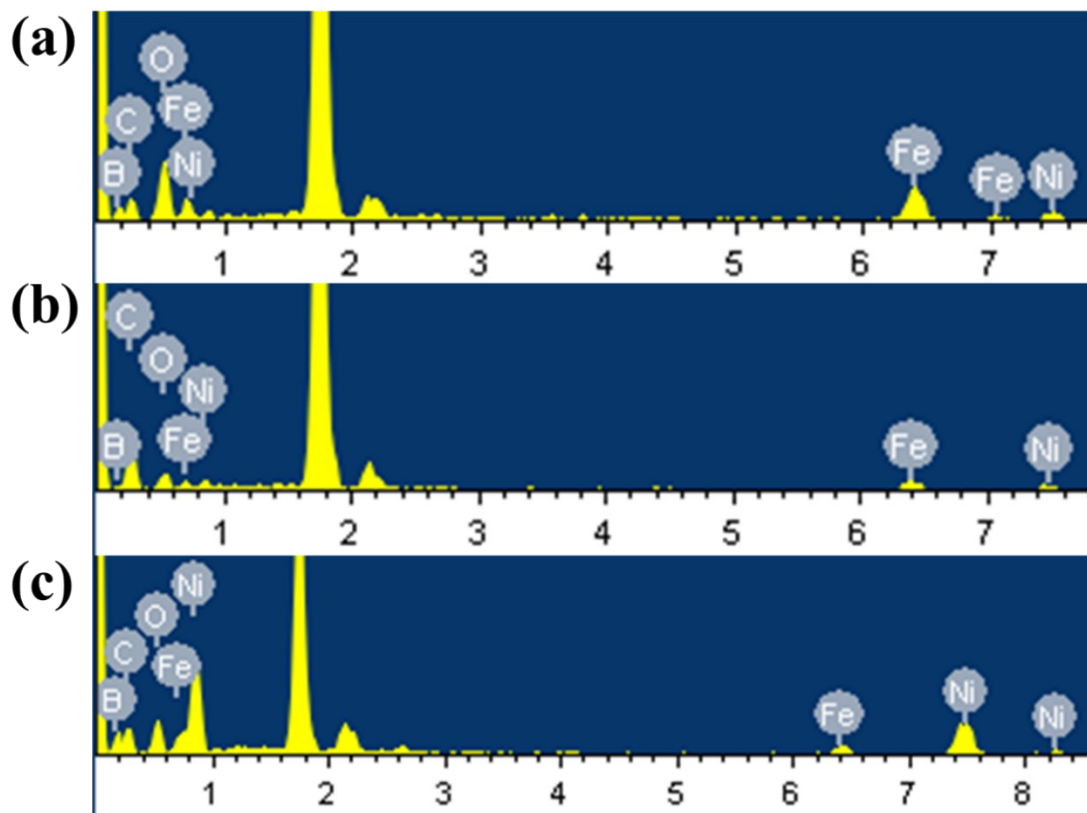


Figure S1. EDS elemental spectra of $\text{Ni}_x\text{Fe}_{1-x}\text{B}-1$, $\text{Ni}_x\text{Fe}_{1-x}\text{B}-2$ and $\text{Ni}_x\text{Fe}_{1-x}\text{B}-3$

Table S1. The content of Fe and Ni according to EDS elemental spectra and ICP-AES analysis.

Samples	Fe (%)		Ni (%)	
	EDS	ICP-AES	EDS	ICP-AES
$\text{Ni}_x\text{Fe}_{1-x}\text{B}-1$	73	68	27	32
$\text{Ni}_x\text{Fe}_{1-x}\text{B}-2$	57	48	43	52
$\text{Ni}_x\text{Fe}_{1-x}\text{B}-3$	13	18	87	82

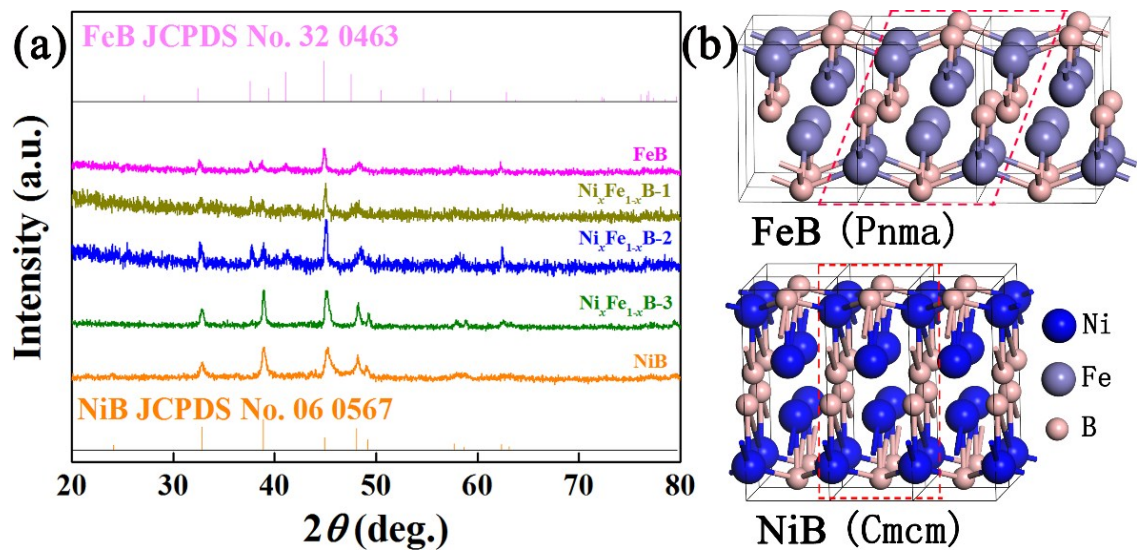


Figure S2. XRD patterns of FeB, $\text{Ni}_x\text{Fe}_{1-x}\text{B}$ -1, $\text{Ni}_x\text{Fe}_{1-x}\text{B}$ -2, $\text{Ni}_x\text{Fe}_{1-x}\text{B}$ -3, NiB and crystal structures of FeB and NiB

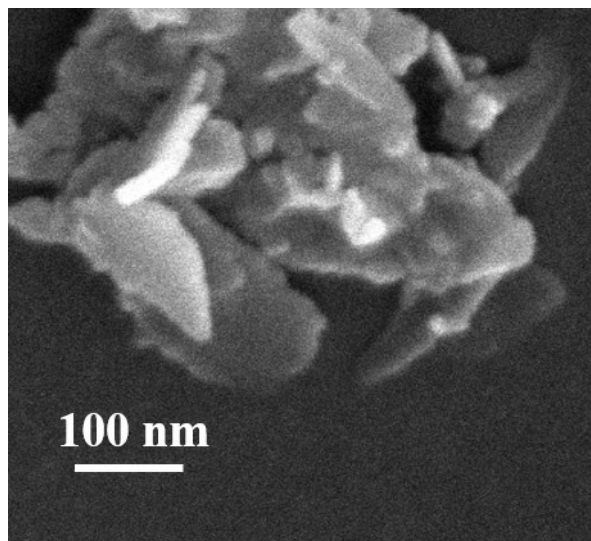


Figure S3. SEM image of $\text{Ni}_x\text{Fe}_{1-x}\text{B}-2$

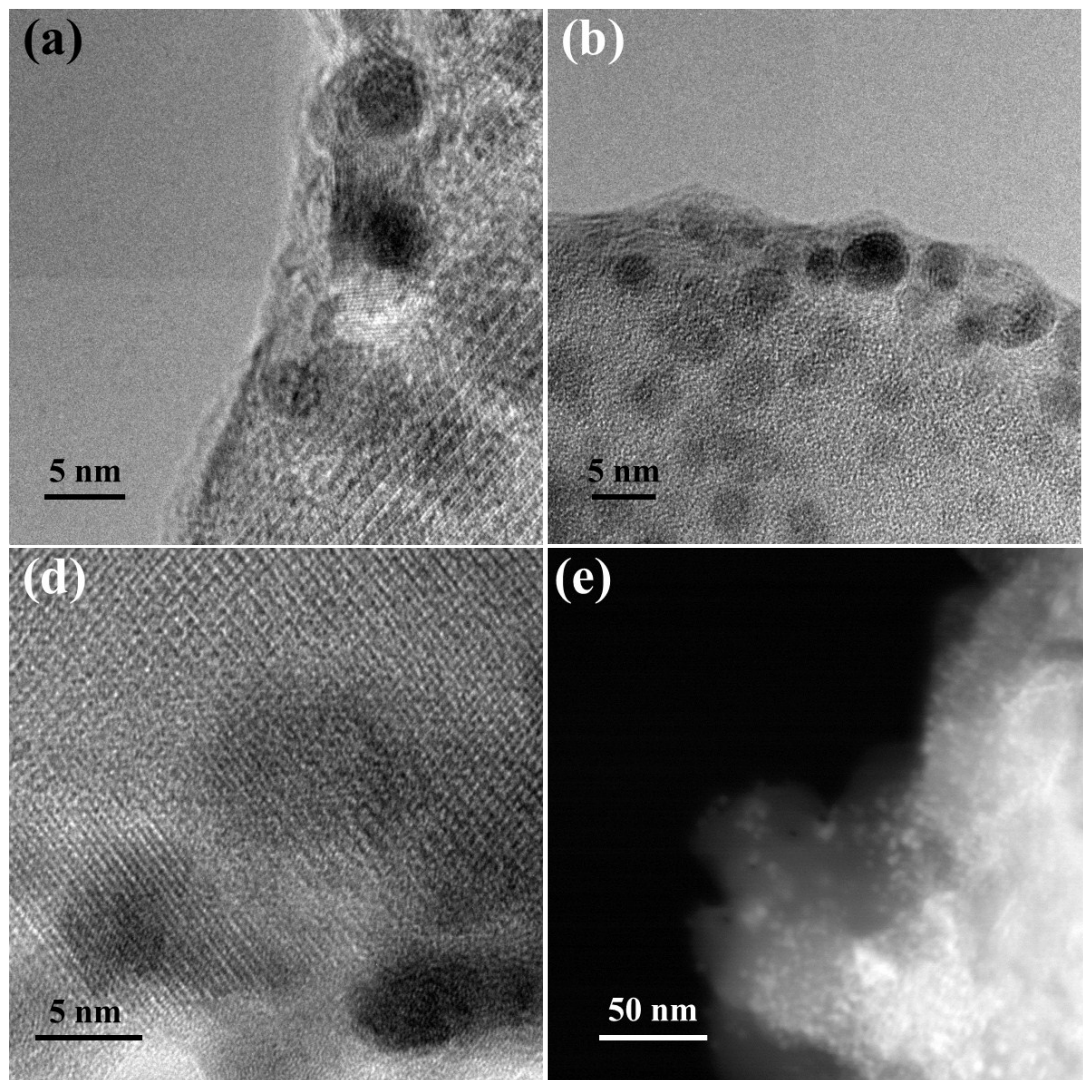


Figure S4. (a-c) TEM images and (e) HAADF image of $\text{Ni}_x\text{Fe}_{1-x}\text{B}-2$

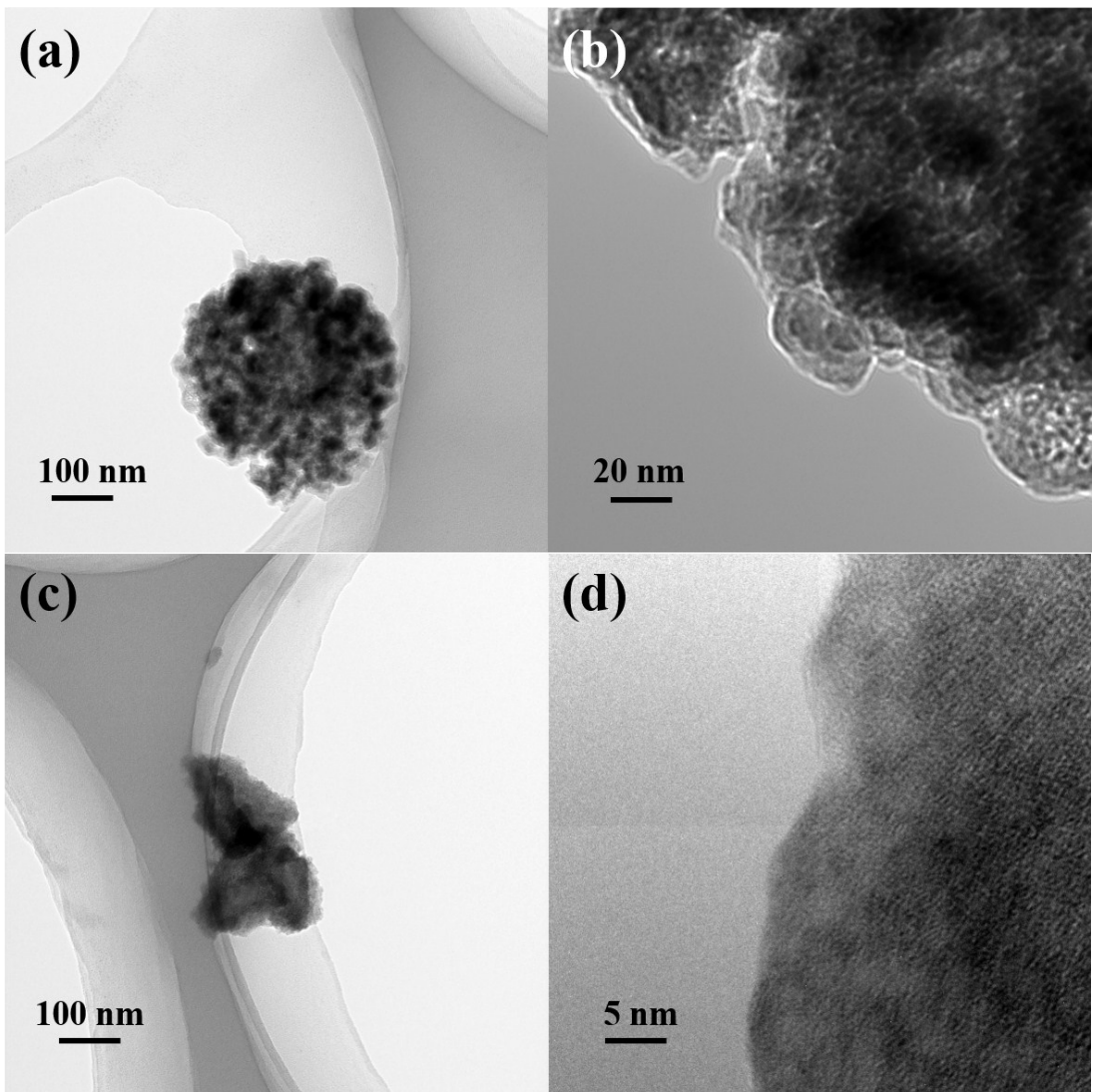


Figure S5. TEM images of (a, b) FeB and (c, d) NiB.

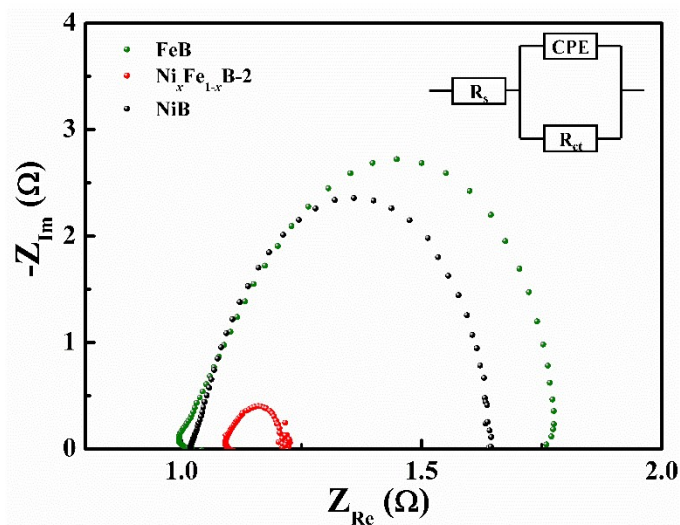


Figure S6. Nyquist plots at -0.065 V vs. RHE

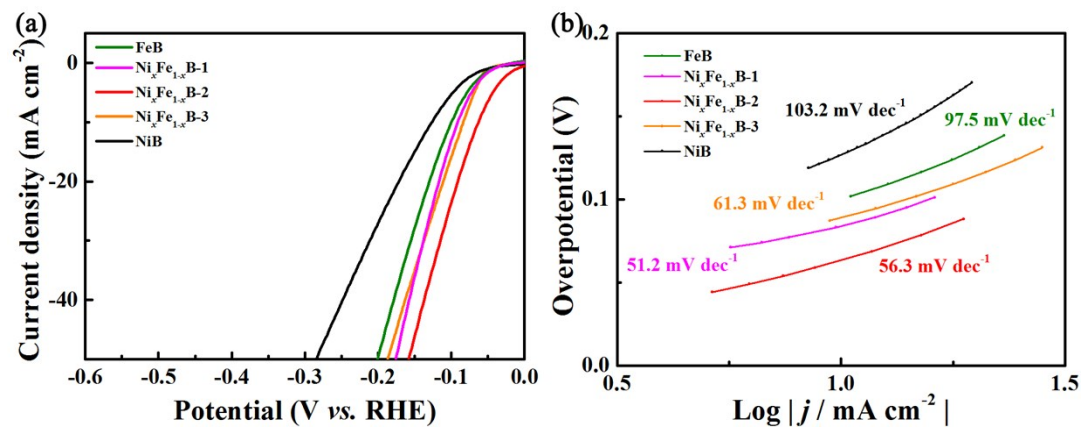


Figure S7. HER performance of FeB, NiB, $\text{Ni}_x\text{Fe}_{1-x}\text{B}$ in 1.0 M KOH. (a) Polarization curves, (b) Tafel plots

Table S2. ΔG_{H^*} of $\text{Ni}_x\text{Fe}_{1-x}\text{B}$ ($x=0, 0.25, 0.5, 0.75$ and 1) with different sites and structures on (001) facet

Site	B-top	Fe-top	Ni-top	Bridge
FeB	-0.248	0.307	N/A	-0.272
$\text{Ni}_{0.25}\text{Fe}_{0.75}\text{B}$	-0.222	0.321	0.544	-0.268
$\text{Ni}_{0.5}\text{Fe}_{0.5}\text{B}$	-0.0270	0.229	0.481	-0.247
$\text{Ni}_{0.75}\text{Fe}_{0.25}\text{B}$ (<i>Pnma</i>)	-0.201	0.215	0.461	-0.285
NiB (<i>Pnma</i>)	-0.431	N/A	0.590	-0.449
$\text{Ni}_{0.75}\text{Fe}_{0.25}\text{B}$ (<i>Cmcm</i>)	-0.486	0.284	0.629	-0.635
NiB (<i>Cmcm</i>)	-0.575	N/A	0.598	-0.584

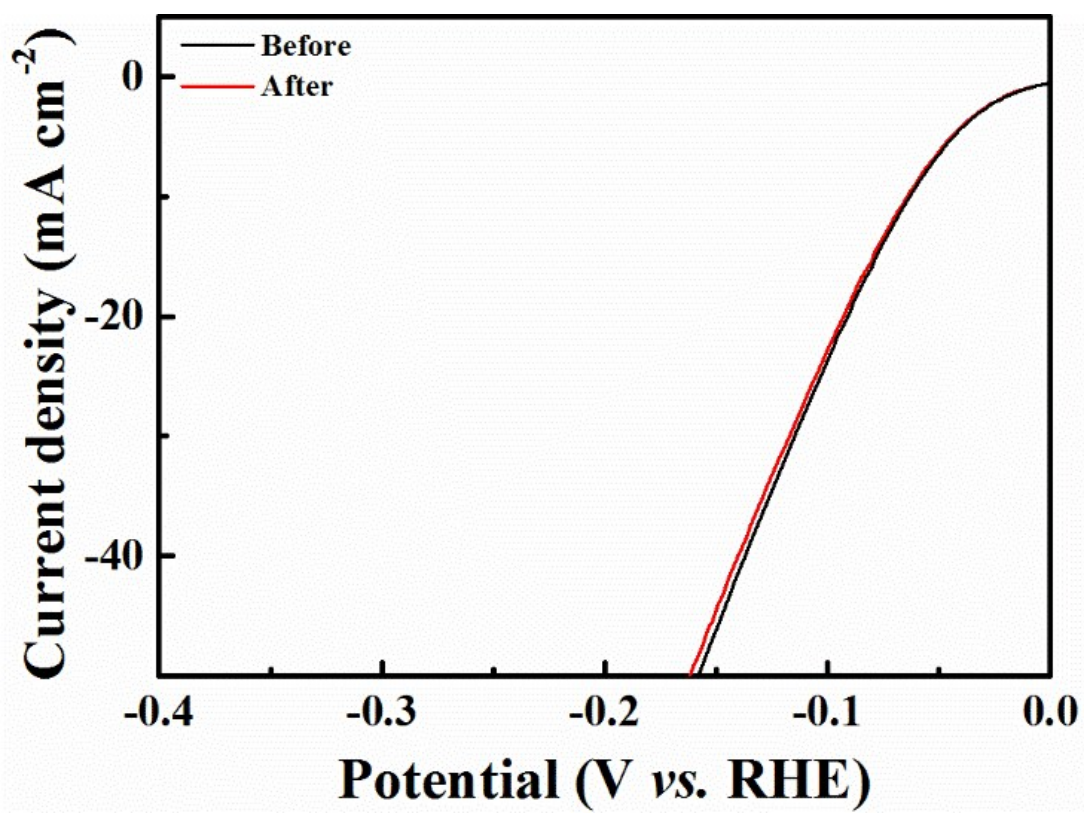


Figure S8. Polarization curve before and after 1000 cycles of a durability test in 1 M KOH

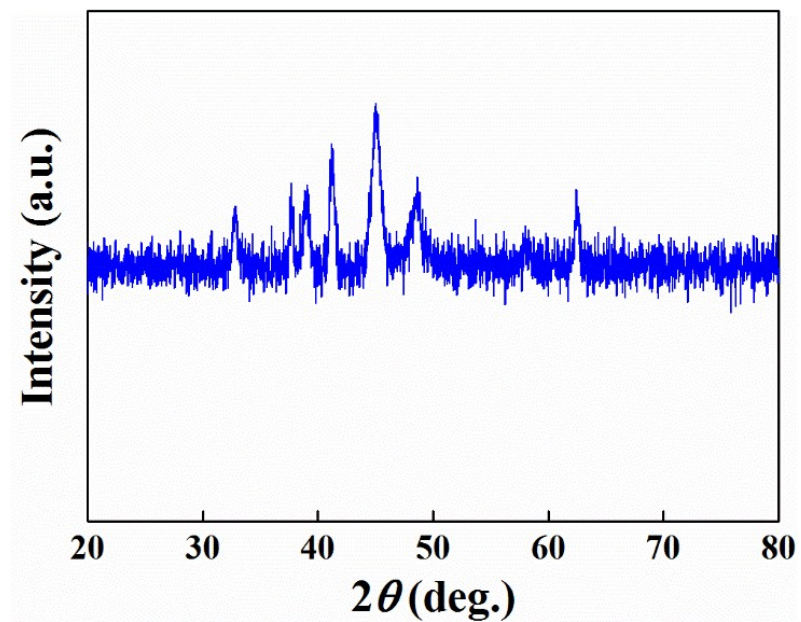


Figure S9. XRD pattern of $\text{Ni}_x\text{Fe}_{1-x}\text{B}-2$ after HER.

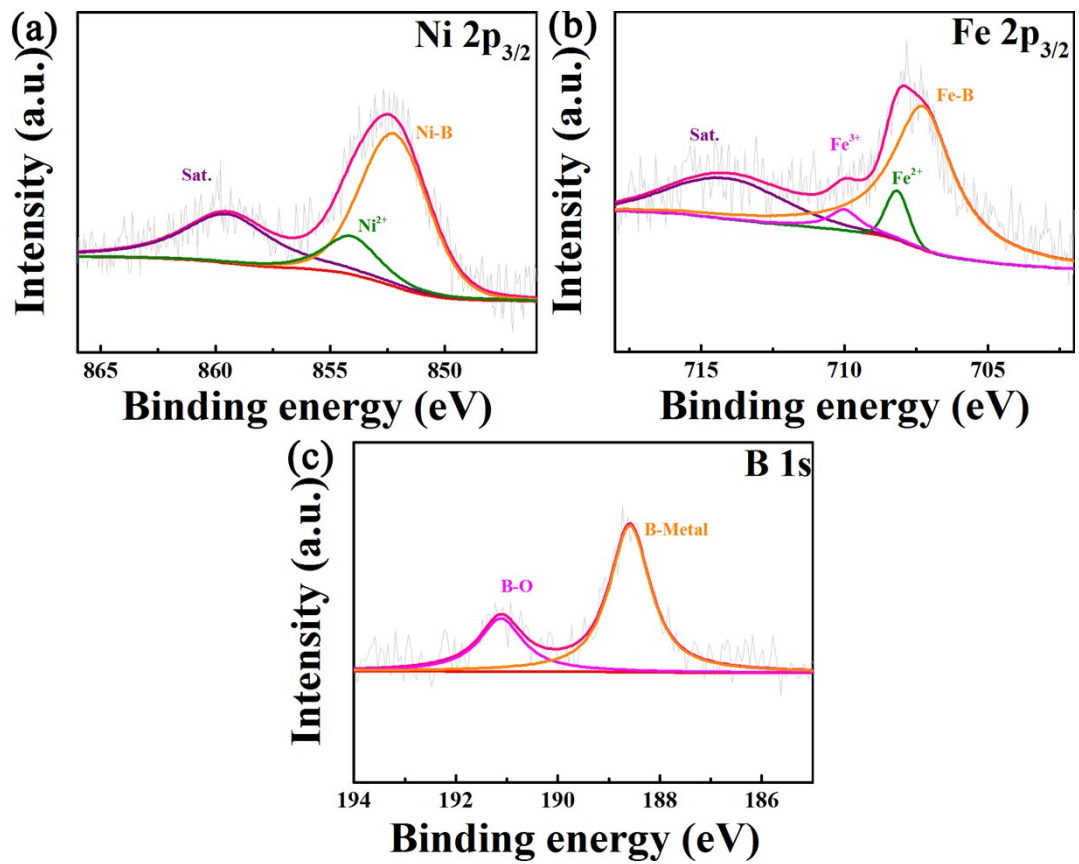


Figure S10. High resolution XPS spectra of (a) Ni 2p_{3/2}, (b) Fe 2p_{3/2}, (c) B 1s of $\text{Ni}_x\text{Fe}_{1-x}\text{B}-2$ after HER.

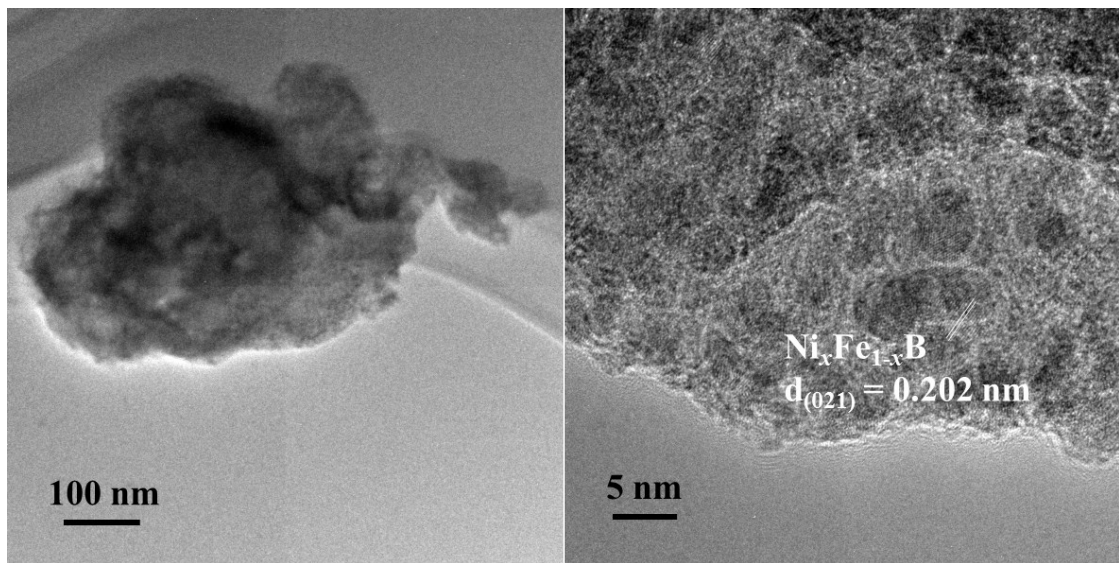


Figure S11. TEM images of Ni_xFe_{1-x}B-2 after HER.

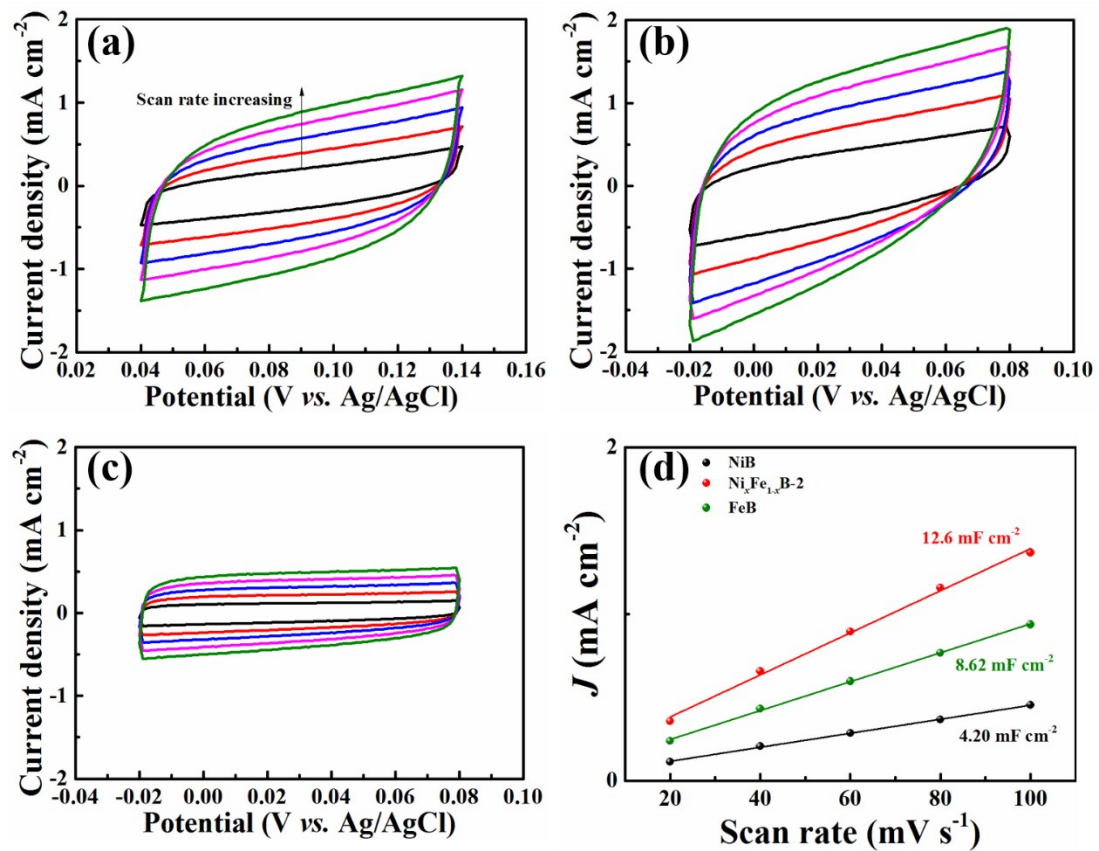


Figure S12. Electrochemical capacitance measurements to determine the surface area of the obtained electrodes in 1 M KOH. The capacitive current density on (a) FeB, (b) $\text{Ni}_x\text{Fe}_{1-x}\text{B-2}$, (c) NiB from double layer charging can be measured from cyclic voltammograms with the scan rates of 20, 40, 60, 80, and 100 mV/s in a potential range where no Faradic reaction occur. d) The measured capacitive current plotted as a function of scan rate.

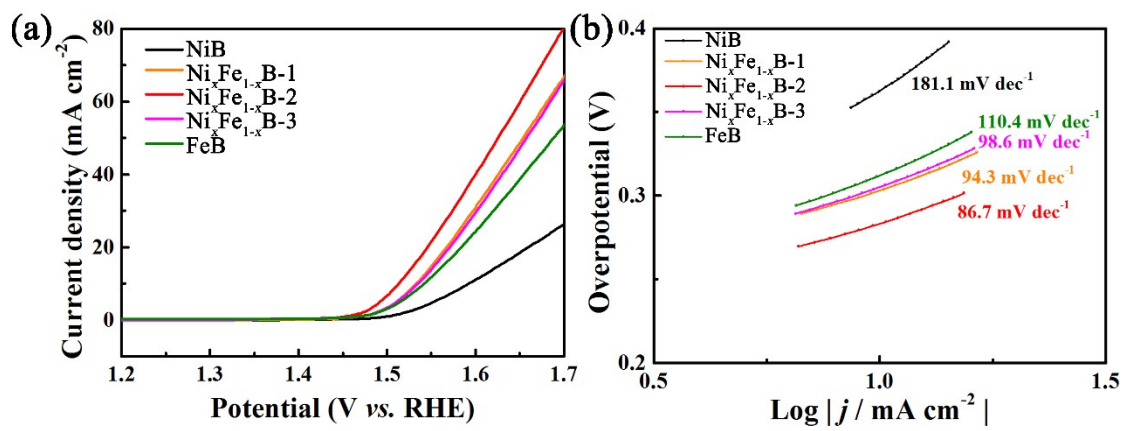


Figure S13. OER performance of FeB, NiB, $\text{Ni}_x\text{Fe}_{1-x}\text{B}$ in 1.0 M KOH. (a) Polarization curves, (b) Tafel plots

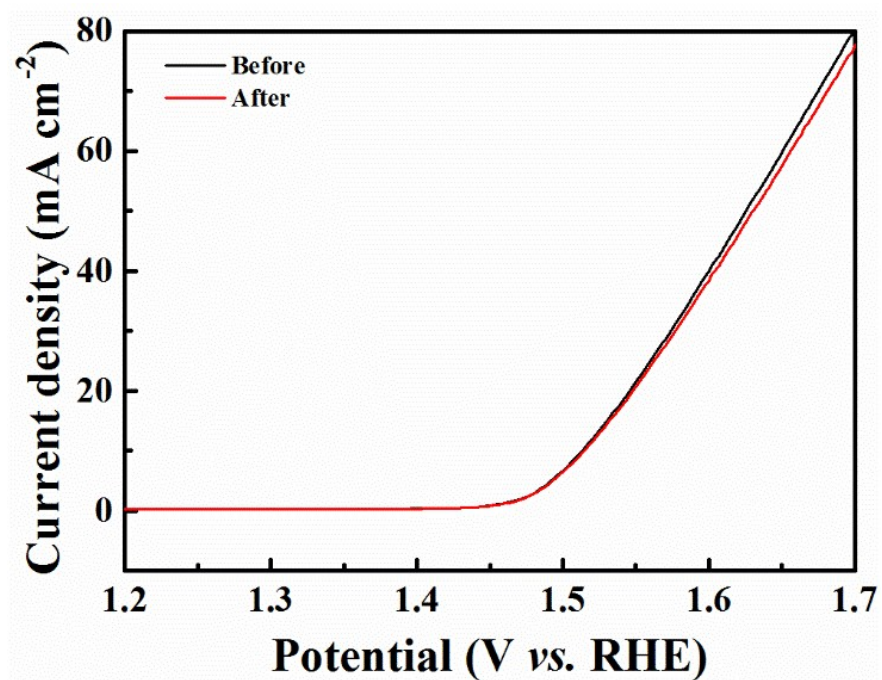


Figure S14. Polarization curve before and after 1000 cycles of a durability test in 1 M KOH

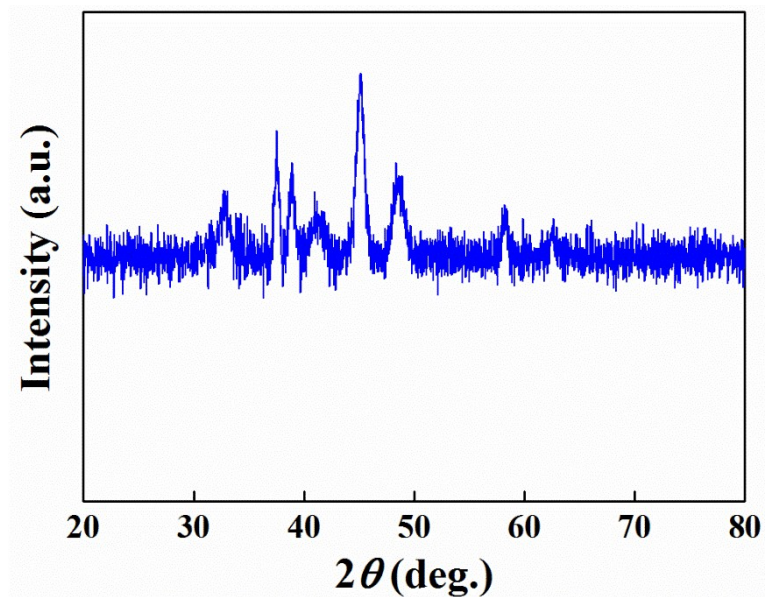


Figure S15. XRD pattern of $\text{Ni}_x\text{Fe}_{1-x}\text{B}-2$ after OER.

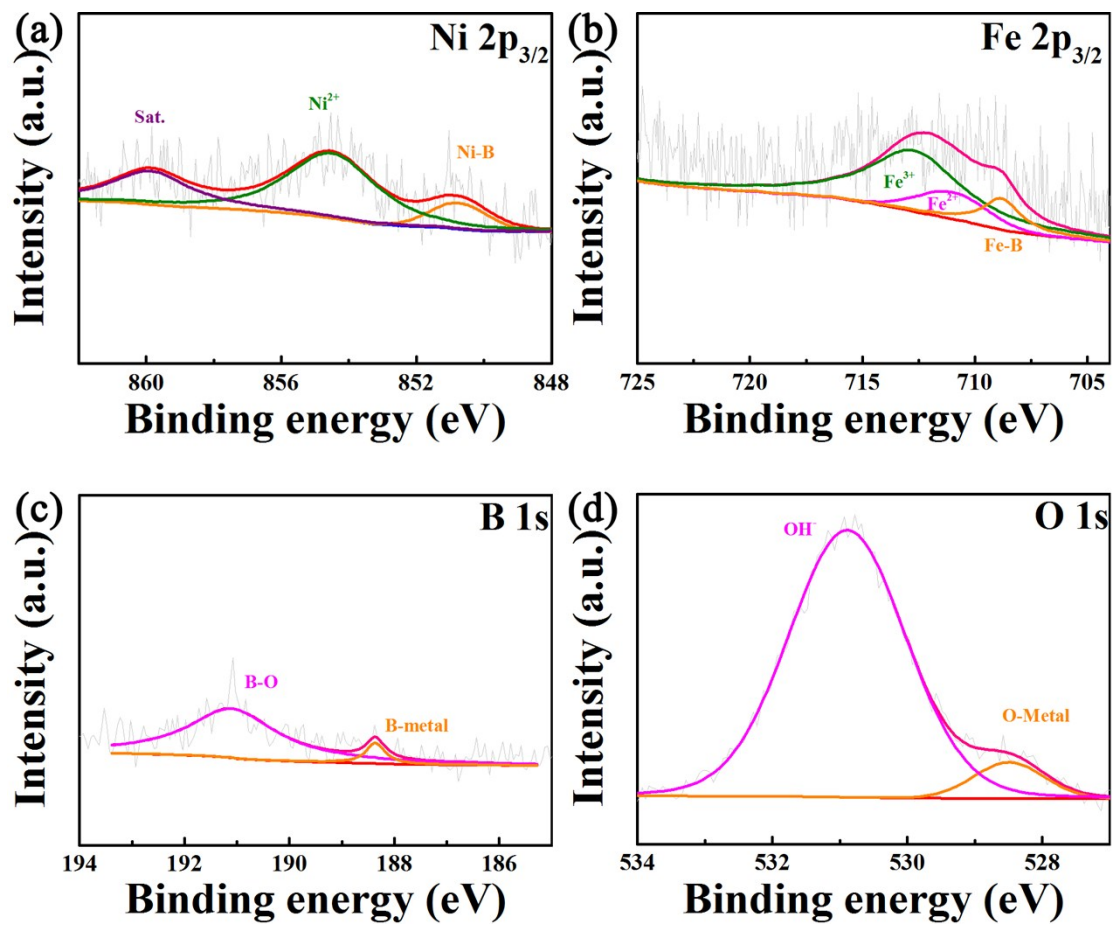


Figure S16. High resolution XPS spectra of (a) Ni 2p_{3/2}, (b) Fe 2p_{3/2}, (c) B 1s (d) O 1s of Ni_xFe_{1-x}B-2 after OER.

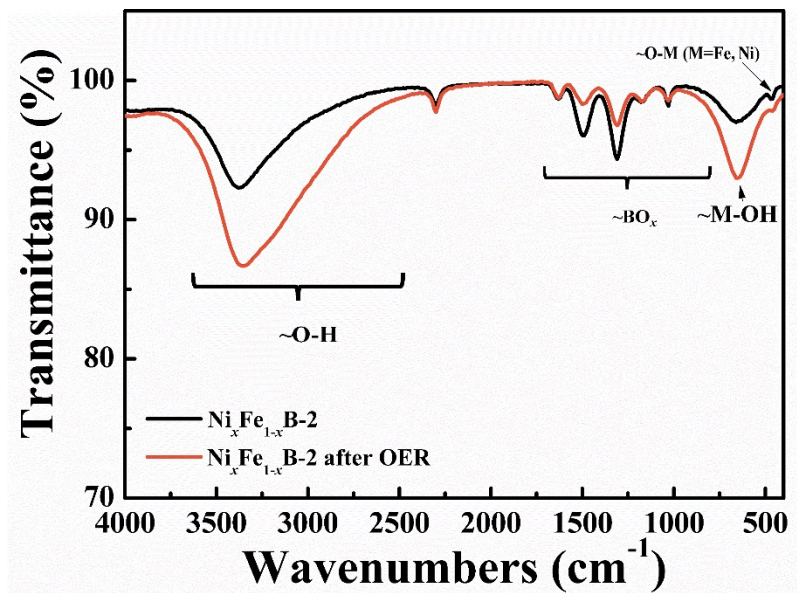


Figure S17. FTIR of $\text{Ni}_x\text{Fe}_{1-x}\text{B}-2$ and $\text{Ni}_x\text{Fe}_{1-x}\text{B}-2$ after OER.

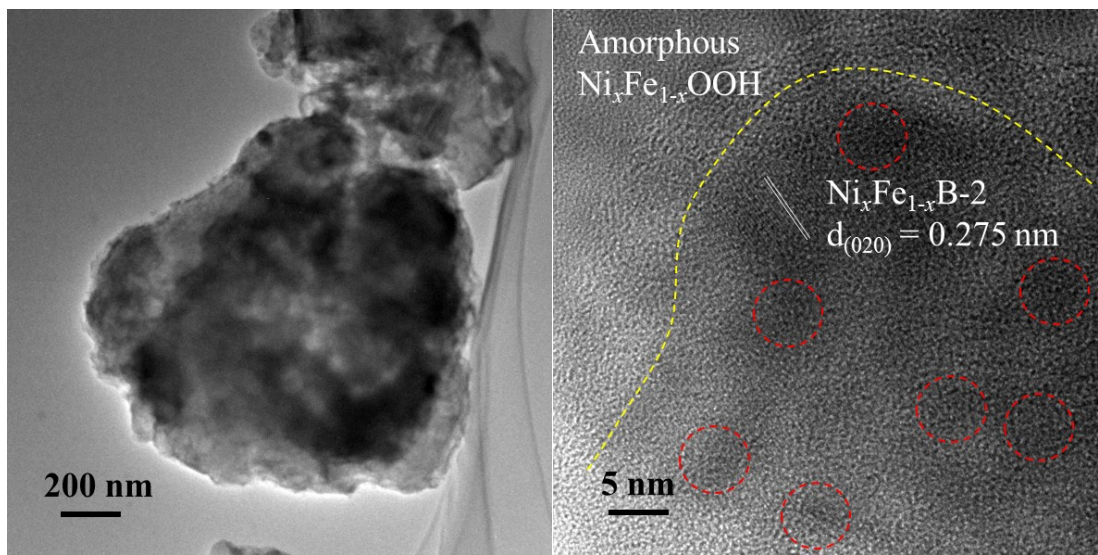


Figure S18. TEM images of Ni_xFe_{1-x}B-2 after OER.

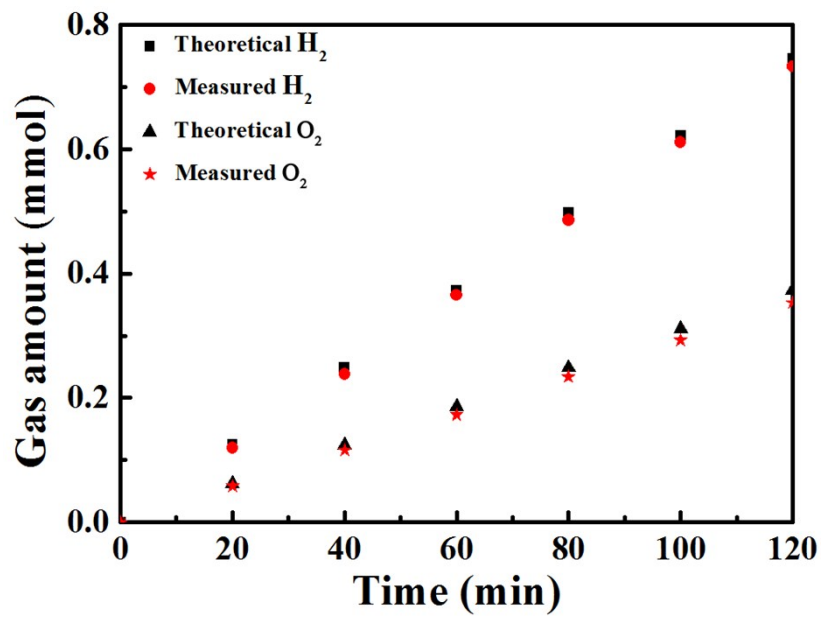


Figure S19. The amount of H₂ theoretically calculated and experimentally measured versus time in 1 M KOH.

Table S3 Comparison of overpotentials for HER at 10 mA cm⁻² (η_{10}) in alkaline electrolyte (1 M KOH) for Ni_xFe_{1-x}B with other recently published highly active HER electrocatalysts

Catalyst	η_{10} (mV)	Tafel slopes (mV dec ⁻¹)	Ref.
FeB ₂	61	87.5	<i>Adv. Energy Mater.</i> DOI:10.1002/aenm.201700513
Ni ₃ S ₂ /VS ₄ nanohorn arrays	177	139	<i>Appl. Catal. B: Environ.</i> DOI:10.1016/j.apcatb.2019.117899
Plasma-doping NiCo LDHs	100	123	<i>Catal. Today</i> DOI:10.1016/j.cattod.2019.04.017
Ni ₂ P/Ni(PO ₃) ₂ /N,S-carbon nanosheet	88	65	<i>Electrochimica Acta</i> DOI: 10.1016/j.electacta.2019.134579
Co-E _x -MoS ₂	89	53	<i>ACS Nano.</i> 2018, 12, 4565.
Ni _{0.51} Co _{0.49} P film	82	43	<i>Adv. Funct. Mater.</i> 2016, 26, 7644
Ni _{0.89} Co _{0.11} Se ₂ MMSN/NF	85	52	<i>Adv. Mater.</i> 2017, 29, 1606521.
Ni ₃ S ₂ -Ni ₂ P/NF	130	77.6	<i>Dalton Trans.</i> 2019, 48, 13466
CoP/CN@MoS ₂	149	88	<i>ACS Appl. Mater. Interfaces</i> DOI:10.1021/acsami.9b11859
CoFeP NFs/NPCNT	132	62.9	<i>Nanoscale</i> , 2019, 11, 17031
Ni _x Fe _{1-x} B	63.5	56.3	This work

Table S4 Comparison of overpotentials for OER at 10 mA cm⁻² (η_{10}) in alkaline electrolyte (1 M KOH) for Ni_xFe_{1-x}B with other recently published highly active HER electrocatalysts

Catalyst	η_{10} (mV)	Tafel slopes (mV dec ⁻¹)	Ref.
FeB ₂	296	52.4	<i>Adv. Energy Mater.</i> DOI:10.1002/aenm.201700513
Ni ₂ P/Ni(PO ₃) ₂ /N,S-carbon nanosheet	190	46	<i>Catal. Today</i> DOI:10.1016/j.cattod.2019.04.017
Plasma-doping NiCo LDHs	273	96	<i>Electrochimica Acta</i> DOI: 10.1016/j.electacta.2019.134579
Ni _{0.51} Co _{0.49} P	239	45	<i>Adv. Funct. Mater.</i> 2016, 26, 7644
NiCoP/NF	280	87	<i>Nano Lett.</i> 2016, 16, 7718
Co ₂ B-500	380	45	<i>Adv. Energy Mater.</i> 2016, 6, 1502313
Ni ₃ Se ₂ -GC	310	79.5	<i>Energy Environ. Sci.</i> 2016, 9, 1771
Mo-CoP	305	56	<i>Nano Energy.</i> 2018, 48, 73
FeCoP UNSAs	260	63	<i>Nano Energy.</i> 2017, 41, 583
CoP/CN@MoS ₂	289	69	<i>ACS Appl. Mater. Interfaces</i> DOI:10.1021/acsami.9b11859
CoFeP NFs/NPCNT	278	39.5	<i>Nanoscale</i> , 2019, 11, 17031
Ni _x Fe _{1-x} B	282	86.7	This work

Table S5 Comparison of overpotentials for electrochemical water splitting at 10 mA cm⁻² (η_{10}) in alkaline electrolyte (1 M KOH) for Ni_xFe_{1-x}B with other recently published highly active HER electrocatalysts

Catalyst	E _{j=10} (mV)	Ref.
FeB ₂	1.57	<i>Adv. Energy Mater.</i> DOI:10.1002/aenm.201700513
Ni ₃ S ₂ /VS ₄ nanohorn arrays	1.57	<i>Appl. Catal. B: Environ.</i> DOI:10.1016/j.apcatb.2019.117899
Ni ₂ P/Ni(PO ₃) ₂ /(N/S)-carbon NS	1.63	<i>Electrochimica Acta</i> DOI: 10.1016/j.electacta.2019.134579
Co ₂ B-500-NG	1.66	<i>ACS Catal.</i> 2017, 7, 469
CoSe ₂ -CC	1.63	<i>Adv. Mater.</i> 2016, 28, 7527
NiCoP-NF	1.58	<i>Nano Lett.</i> 2016, 16, 7718
Ni ₃ S ₂ -Ni ₂ P/NF	1.58	<i>Dalton Trans.</i> 2019, 48, 13466
CoP/CN@MoS ₂	1.61	<i>ACS Appl. Mater. Interfaces</i> DOI:10.1021/acsami.9b11859
CoFeP NFs/NPCNT	1.56	<i>Nanoscale</i> , 2019, 11, 17031
Ni _x Fe _{1-x} B	1.57	This work